LaConte, D. D. Thomas, *Proc. Natl. Acad. Sci. U.S.A.* **95**, 2944 (1998).
45. G. Woehlke *et al.*, *Cell* **90**, 207 (1997).
46. The main polymer binding elements of kinesin (loop 12) and myosin (lower 50 kD domain) as well as "secondary" polymer binding sites (kinesin, loop 8/β5; myosin, upper 50 kD domain) are positioned similarly with respect to the common cores (*45*). As a result, the catalytic cores of kinesin and myosin are oriented in an overall similar position with respect to the axes of microtubule and actin filaments (Fig. 4A). Switch II and the relay helix are connected to the main polymer binding site, whereas switch I is located close to the secondary polymer binding site. These two switch regions probably affect the conformations of their adjacent polymer binding elements.
47. C. Veigel *et al.*, *Nature* **398**, 530 (1999).
48. A three-dimensional view of a pocket that constitutes a docking site for conserved residues from the kinesin neck linker (e.g., Ile^{325} in Fig. 2) can be seen at *Science* Online (www.sciencemag.org/feature/data/1049155.shl).
49. R. A. Walker, E. D. Salmon, S. A. Endow, *Nature* **347**, 780 (1990).
50. H. B. McDonald, R. J. Stewart, L. S. Goldstein, *Cell* **63**, 1159 (1990).
51. A. L. Wells *et al.*, *Nature* **401**, 505 (1999).
52. K. Hirose, A. Lockhart, R. A. Cross, L. A. Amos, *Proc. Natl. Acad. Sci. U.S.A.* **93**, 9539 (1996).
53. The ATP- and ADP-bound states are tight and weak binding microtubule states, respectively, for both Ncd and conventional kinesin (*59, 72*). Like other myosins, the ADP-bound state is a tight binding state for myosin VI (*51*).
54. Although the kinesin neck linker (interrupted β strand) and the Ncd neck (coiled-coil helix) differ in structure and emerge from the COOH- and NH_2-termini of the catalytic core, both necks dock in a comparable configuration along the catalytic core and therefore may respond to similar cues from the active site (*41*). In contrast to kinesin, the two heads of Ncd are held together tightly by the neck coiled coil, which may restrain the Ncd dimer from forming a two-head-bound intermediate and moving processively along the microtubule.
55. Other examples of motors with different amplifiers include *Toxoplasma* myosin XIV, which lacks a long lever helix (*73*) and may operate using only a "converter-based" amplifier. Many types of kinesin necks also have evolved, some of which may stimulate mechanical disassembly of microtubules (*74*).
56. A. D. Mehta *et al.*, *Nature* **400**, 590 (1999).
57. R. J. Stewart, J. Semerjian, C. F. Schmidt, *Eur. Biophys. J.* **27**, 353 (1998).
58. I. M. Crevel, A. Lockhart, R. A. Cross, *J. Mol. Biol.* **273**, 160 (1997).
59. E. Pechatnikova and E. W. Taylor, *Biophys. J.* **77**, 1003 (1999).
60. An interesting and unusual form of "processive" motion was discovered for a truncated kinesin KIF1A monomer, which displays biased one-dimensional diffusion along the microtubule (*75*). The monomeric motor domain of muscle myosin (S1) was also reported to take several consecutive steps along actin (*76*). The motility models proposed in those studies differ from the models presented here.
61. D. D. Hackney, *Proc. Natl. Acad. Sci. U.S.A.* **91**, 6865 (1994).
62. Y.-Z. Ma and E. W. Taylor, *J. Biol. Chem.* **272**, 724 (1997).
63. S. P. Gilbert, M. L. Moyer, K. A. Johnson, *Biochemistry* **37**, 792 (1998).
64. Occasionally in the prestroke (no nucleotide, or ADP-bound) state, the neck linker may extend forward by thermal motion and allow the second head to bind to the forward tubulin and release its ADP. This may account for the fact that ADP release from the partner head in this intermediate microtubule-bound state is faster ($\sim 0.5\ s^{-1}$) relative to kinesin in solution ($0.01\ s^{-1}$). However, ATP-driven neck linker docking further increases the ADP release rate from the partner head to $>100\ s^{-1}$ (*62, 63*).
65. L. Romberg, D. W. Pierce, R. D. Vale, *J. Cell Biol.* **140**, 1407 (1998).
66. In the presence of actin, ADP release is the rate-limiting step in myosin V's ATPase cycle (*67, 77*). Thus, relative to muscle myosin, myosin V spends more time in a strongly bound state. This helps to maintain the two-head-bound intermediate by preventing the rapid release of the trailing head upon the completion of its power stroke (Fig. 5).
67. M. Rief *et al.*, in preparation.
68. P. D. Boyer, *Annu. Rev. Biochem.* **66**, 717 (1997).
69. A. Houdusse and C. Cohen, *Structure* **4**, 21 (1996).
70. R. B. Case, S. Rice, C. L. Hart, B. Ly, R. D. Vale, *Curr. Biol.* **10**, 157 (2000).
71. R. Cooke, *Curr. Biol.* **9**, R773 (1999).
72. A. Lockhart and R. A. Cross, *EMBO J.* **13**, 751 (1994).
73. M. B. Heintzelman and J. D. Schwartzman, *J. Mol. Biol.* **271**, 139 (1997).
74. A. Desai, S. Verma, T. J. Mitchison, C. E. Walczak, *Cell* **96**, 69 (1999).
75. Y. Okada and N. Hirokawa, *Science* **283**, 1152 (1999).
76. K. Kitamura, M. Tokunaga, A. H. Iwane, T. Yanagida, *Nature* **397**, 129 (1999).
77. E. M. De La Cruz, A. L. Wells, S. S. Rosenfeld, E. M. Ostap, H. L. Sweeney, *Proc. Natl. Acad. Sci. U.S.A.* **96**, 13726 (1999).
78. Unlike a robotic machine, the working stroke is likely to vary somewhat from one enzymatic cycle to the next, because the motor can begin its power stroke from a variety of conformations (not depicted in Fig. 4). For example, in myosin's prestroke state (ADP-Pi), the catalytic core can bind weakly to actin in several orientations, and the lever arm may be tilted at various angles relative to the core (*20, 43, 44*). Similarly, in a kinesin monomer, the neck linker is mobile in the pre–power stroke state (*26*). Thus, the power stroke in both kinesin and myosin appears to involve a "disordered-to-ordered" transition.
79. Because of space constraints, we can cite relatively few articles; we regret not being able to acknowledge many of the important contributions in this field. We thank G. Johnson, A. Lin, E. Sablin, and B. Sheehan for figure preparation. We are also grateful to C. Cohen, R. Cooke, R. Fletterick, S. Rice, L. Sweeney, E. Taylor, and K. Thorn for many stimulating discussions and for providing comments on the manuscript.

REVIEW

Motility Powered by Supramolecular Springs and Ratchets

L. Mahadevan[1] and P. Matsudaira[2,3]*

Not all biological movements are caused by molecular motors sliding along filaments or tubules. Just as springs and ratchets can store or release energy and rectify motion in physical systems, their analogs can perform similar functions in biological systems. The energy of biological springs is derived from hydrolysis of a nucleotide or the binding of a ligand, whereas biological ratchets are powered by Brownian movements of polymerizing filaments. However, the viscous and fluctuating cellular environment and the mechanochemistry of soft biological systems constrain the modes of motion generated and the mechanisms for energy storage, control, and release.

In his famous letter of 1676 to the Royal Society, the 17th-century microscopist Leeuwenhoek (*1*) described how the body of a simple unicellular organism, probably a vorticellid, was connected by a slender stalk to a fragment of leaf and wrote this about its movement: ". . .their whole body then lept towards the globul of the tayl. . .and unwound again. This motion of extension and contraction continued a while . . . "

This example of motility, the retraction by the stalk of peritrich ciliates, is caused not by the sliding action of a motor protein but by a spring that operates according to a simple mechanism: the entropic collapse of polymeric filaments. Although they are regarded as unusual engines for motility, springs and ratchets composed of filaments and tubules power many of the largest, fastest, and strongest cellular and molecular movements. Just as muscles magnify forces and movements by a clever geometrical hierarchy, these unusual mechanochemical engines (*2*) use a similar principle: Small changes in a protein subunit are amplified by their linear arrangement in filaments and bundles. From the biochemical and physical characteristics of several molecular springs and ratchets we will argue that they represent ancient and commonplace eukaryotic molecular engines.

Supramolecular Springs—Conformation Changes Driven by Ion Binding

Biological springs are active mechanochemical devices that store the energy of conformation in certain chemical bonds that act as

[1]Department of Mechanical Engineering, [2]Department of Biology and Division of Bioengineering and Environmental Health, Massachusetts Institute of Technology, [3]Whitehead Institute for Biomedical Research, Cambridge, MA 02142, USA.

*To whom correspondence should be addressed. E-mail: matsu@wi.mit.edu

latches (*3*). In the absence of an external force, the potential energy is released and converted into mechanical movement when the chemical bonds are broken.

The contractile avoidance reaction described by Leeuwenhoek in 1676 is a dramatic example of an active mechanochemical spring. The body of a vorticellid is attached to a leaf by a long slender stalk (Fig. 1). Within the stalk lies a rodlike helical cytoplasmic organelle, the spasmoneme. In its extended state, the spasmoneme is 2 to 3 mm long, depending on the species of ciliate. When exposed to calcium but no external energy source, the spasmoneme contracts in a few milliseconds to 40% of its length at velocities approaching 8 cm/s (*4*, *5*). Based on the hydrodynamics, the force of contraction is on the order of a millidyne, whereas the power generated is a few milliergs per second. In terms of specific power per unit mass, the spasmoneme is among the most powerful biological engines (Table 1).

How might this engine work? The spasmoneme is a bundle of filaments, each 2 nm in diameter (Fig. 1B). Although the structures of a filament and of the bundle are unknown, birefringence measurements (*4*) show that the extended spasmoneme is composed of roughly aligned but weakly cross-linked filaments. Shrinkage and swelling of the spasmoneme in the absence or presence of calcium (*6*) suggest that contraction is driven by the imbalance between osmotic and entropic forces, much as in a polyelectrolyte gel (*7*). Hoffmann-Berling proposed that energy is stored by the electrostatic repulsion between negatively charged filaments (*8*). In the presence of calcium, the highly charged state is neutralized so that the spasmoneme filaments collapse entropically and condense into an isotropic state. Implicated in calcium binding and perhaps contraction is spasmin, the major spasmoneme protein and a member of the EF-hand superfamily of calcium-binding proteins (*9*). Contraction is amplified by the number and linear arrangement of the subunits in the polymeric network that form the contracting organelle. Because the spasmoneme is helical, it rotates during contraction. This interplay between twisting (or bending) and extension is a recurring theme in all mechanochemical springs.

The rapidity of contraction may be explained by the mechanism of calcium release in the stalk. Calcium stored in a membrane compartment that lies along the length of the stalk is globally released from the stores, and the contraction rate becomes limited by calcium diffusion across the membrane (which typically occurs in a few milliseconds). The process reverses during extension of the stalk, as intracellular membrane compartments sequester calcium ions. However, extension is limited by the slow rate of dissociation of the calcium ions, and a few seconds are required to attain full length.

Although the mechanism of contraction is plausible and is consistent with experiments, some key biochemical and structural issues remain unresolved. Most important, because a spasmoneme filament has not been reconstituted from purified proteins, we do not know whether spasmin is indeed the contractile filament. In addition, the extent of the electrostatic changes induced by calcium and the triggering process are unresolved. Ironically perhaps, three centuries after Leeuwenhoek's observations, the technological quest for soft actuators (*10*) such as artificial muscles (*11*, *12*) is based on essentially the same geometrical and physical principles that power these biological machines.

A spasmoneme-like spring is implicated in other movements. The nuclear movements of unicellular protists involve a spasmin homolog, centrin (*13*): a ubiquitous component of centrioles and basal bodies and part of a filamentous contractile rootlet of unicellular flagella. The sequence homology between spasmin and centrin and centrin's presence in a fiberlike structure suggest that a spasmin-like engine may power several basic steps in mitosis, including duplication of the centrioles and spindle pole body (*14*, *15*).

A very different spring is involved in initiating the process of fertilization in some marine invertebrates, whose eggs are covered by a jelly that presents a soft barrier to fertilization. To penetrate the jelly coat, a sperm cell extends a 60-μm-long finger, the acrosomal process, which fuses with the egg plasma membrane (*16*). In sperm cells of the horseshoe crab *Limulus polyphemus*, a bundle of actin filaments initially lies coiled around the base of the nucleus (Fig. 2). At fertilization, the bundle uncoils and slides through a tunnel in the nucleus forming the acrosomal process.

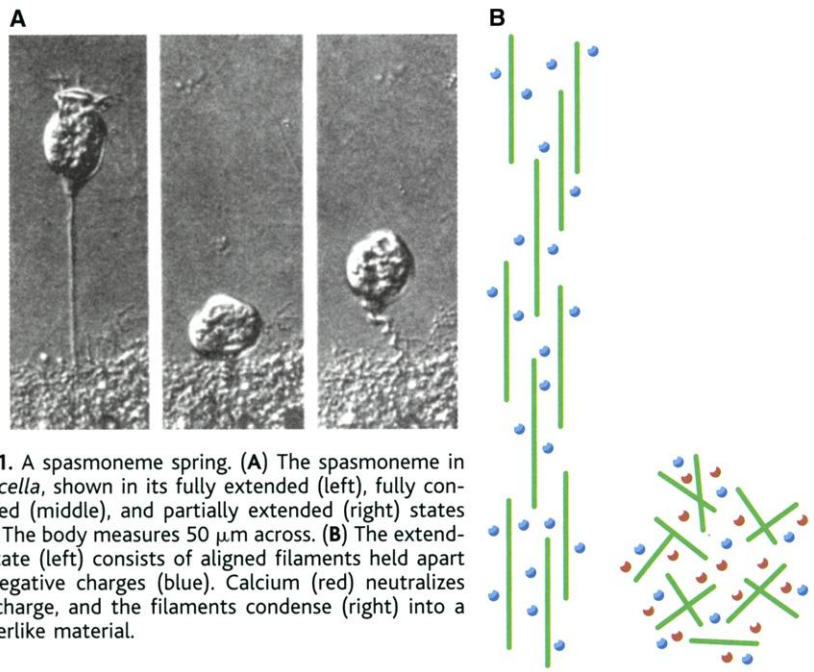

Fig. 1. A spasmoneme spring. (**A**) The spasmoneme in *Vorticella*, shown in its fully extended (left), fully contracted (middle), and partially extended (right) states (*52*). The body measures 50 μm across. (**B**) The extended state (left) consists of aligned filaments held apart by negative charges (blue). Calcium (red) neutralizes the charge, and the filaments condense (right) into a rubberlike material.

Table 1. Engines. The performance of various cellular engines is compared with thermal energy (*kT*) and an automobile engine. Calculations for the specific power are based on the molecular weight of the smallest unit of the engine. Thus, molecular motors and polymerization-based engines are more powerful than the cellular structures in which they are found; for example, compare myosin to striated muscle.

Engine	Velocity ($\mu m\ s^{-1}$)	Force (dynes)	Specific power ($erg\ s^{-1}\ g^{-1}$)
kT (thermal energy)	–	4×10^{-7} dyne nm	
Actin polymerization (*40*)	1	1×10^{-6}	1×10^{9}
Microtubule polymerization (*49*)	0.02	4×10^{-7}	5×10^{8}
Myosin II (*55*)	4	1×10^{-6}	2×10^{8}
Kinesin (*56*)	1	6×10^{-7}	7×10^{7}
Vorticellid spasmoneme (*4*)	8×10^{4}	1×10^{-3}	4×10^{7}
Typical passenger car engine (*57*)			3×10^{6}
Striated muscle (*57*)			2×10^{6}
Bacterial flagellar motor (*58*, *59*)	100 Hz	4.5×10^{-11} dyne cm	1×10^{6}
Thyone acrosomal reaction (*60*)	6–9	5×10^{-4}	1×10^{5}
Limulus acrosome reaction	10	1×10^{-6}	1×10^{4}
Eukaryotic flagellum (*57*)			3×10^{2}
Mitotic spindle (*57*)	2	1×10^{-5}	

The reaction is completed within a few seconds. Two remarkable features characterize this phenomenon. First, the extension does not involve a myosin motor or actin polymerization. Second, the bundle is crystalline in its coiled and uncoiled states (*17*, *18*).

Although the energetics, biochemistry, and dynamics of this machine are only partially resolved, structural analysis of the coil shows that the actin cross-linking protein scruin captures actin filaments in a slightly overtwisted state—0.23° per actin subunit (*17*, *18*). Our biochemical studies (*19*, *20*) on scruin suggest that calcium-dependent conformation changes in scruin could unlatch the overtwisted filaments; the subsequent untwisting of the filaments is coupled to the extension of the bundle (Fig. 2). Here, the geometric magnification of subtle subunit conformation changes is achieved in yet another ingenious way, by combining the shear induced by the sliding and twisting of filaments in the bent bundle and the chirality of actin filaments. Because the actin bundle remains crystalline before and after the reaction, we speculate that the change in twist of the filaments is propagated along the bundle in the same way as a defect moves through a crystal. Owing to the wealth of information on the structure of actin filaments and their organization into a bundle, this system affords the possibility of bridging the connection between structure and macromolecular function. However, two key technical advances—the purification of coils and the development of an in vitro assay—are required to identify the mechanism of latching and to measure the energy stored in the coil.

More generally, a change in actin twist is emerging as a major mechanism for modulating the stability of a filament and perhaps its interactions with other proteins. Small actin-binding proteins, such as actin depolymerizing factor (ADF) and cofilin, depolymerize actin filaments by weakening the lateral contacts between subunits. Image reconstructions show a profound [4° to 5° per subunit (*21*)] untwisting at sites of cofilin binding. An unresolved question is whether the change in twist is propagated along the filament.

Soft springs are not limited to eukaryotes; during infection of a bacterium by T-even phages, phage DNA is injected into the cell by contraction of the tail sheath of the virus. Image analysis reveals large changes in the phage after contraction when the sheath is compressed (*22*). Contraction begins when contact with a bacterium by the phage tail fibers is transmitted to the energetically metastable sheath through a large rotation in the phage base plate. This rotation nucleates a conformation change that propagates up the sheath of the tail (*23*–*25*), shortens the tail, and drives the tail core into the bacterium. The source and magnitude of the energy that drives this movement is unknown at present.

Supramolecular Ratchets—Movement Driven by Polymerization-Induced Growth

The morphology and motility of a cell are determined by a dynamic rearrangement of cytoskeletal polymers. For example, to generate forces that move the cell body, actin polymerization is spatially and temporally coordinated at the membrane of an extending lamellipodium. This bias in polymerization is associated with the addition of adenosine triphosphate (ATP)–actin subunits to the elongating end of the filament and with the conformation change associated with nucleotide hydrolysis. However, unlike in motors or springs, motion in these systems is simply due to growth; the role of conformation changes is more subtle and is associated with changing the kinetics of polymerization. The growing filaments may then be bundled or cross-linked to form a gel that is able to provide the motive force for movement. This model of motility is often referred to as a Brownian ratchet (*26*, *27*), because it involves the mechanochemical rectification of the random motions of the filaments in the presence of energy (*28*), much as a mechanical pawl and ratchet mechanism can rectify oscillatory motion (Fig. 3) (*29*). It should be stressed that these ratcheting motions have never been directly observed in a biological setting.

In a wonderful example of convergent evolution, the acrosome reaction has used an actin spring and an actin Brownian ratchet. Tilney showed that actin polymerization performs work in the acrosome reaction of marine echinoderm sperm cells (*30*). Unlike the preformed actin bundle of the horseshoe crab sperm, the actin bundle in the acrosomal process of an echinoderm sperm cell is assembled de novo from a nonfilamentous pool of actin subunits. The preferred site for subunit addition is at the distal end of a filament; consequently, the growing bundle pushes the plasma membrane from the cell body to form a 60-μm-long acrosomal process (*31*). A similar bundle of actin forms during the acrosome reaction of the parasite *Toxoplasma gondi* (*32*).

How is a polymerization-based engine controlled? In the quiescent cell, the actin subunits are kept in an unpolymerized state as a complex with profilin, and the engine is off. Changes in intracellular pH dissociate the complex; the high concentration (10 mM) of unpolymerized actin provides the chemical potential that drives the assembly of filaments through mass action. In this example, the monomer/polymer equilibrium controls polymerization just like an imbalance of ions across a cell membrane drives transport. The location and orientation of nucleating sites and the polarity of actin filaments channel the forces induced by polymerization (*33*); however, a competing osmotic pressure model cannot be ruled out (*34*).

This intracellular machinery for motility is coopted by some viruses and bacteria for their own motility during the spread of infection to other cells. The most studied of these systems is associated with the pathogenic bacteria *Listeria monocytogenes*, which powers its way through the cell by polymerizing a bundle of host cell actin filaments (Fig. 3B) (*35*). The velocity of the bacterium matches the rate of actin polymerization (*36*), and the bundle remains stationary, enmeshed in the host cytoskeleton.

Actin polymerization is nucleated on the posterior end of the bacterium by factors that include a bacterial protein, ActA, and host cell actin-binding proteins, including fimbrin, Arp2/3, and ADF. Because of the asymmetric location of the polymerization nucleation sites on the bacterium, the growth of actin is also asym-

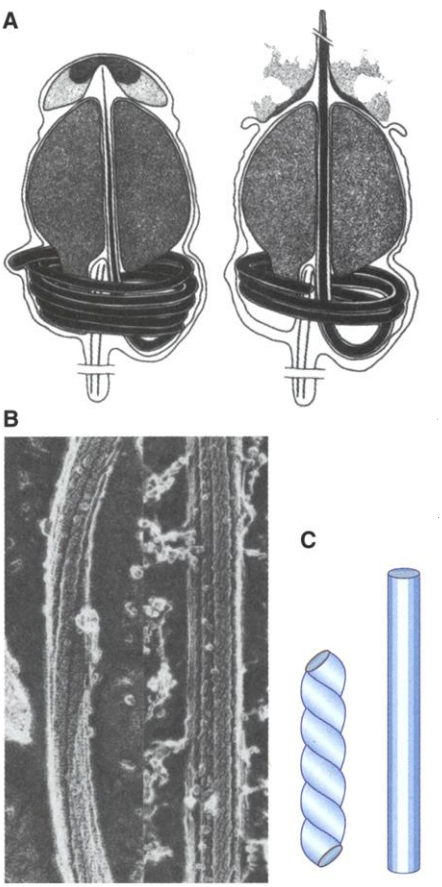

Fig. 2. An actin spring. (**A**) The actin bundle in a *Limulus* sperm is coiled (left) around the base of the nucleus and extends through a nuclear channel at activation (right) (*17*). The sperm head is 3 μm in diameter. (**B**) A portion of the coil (left) shows bends in the bundle and the superhelicity of the bundle. In contrast, the filaments in the extended bundle (right) are straight and unwound (*53*). (**C**) The coiled bundle stores energy in an overtwisted filament (left). When unlatched by calcium, the change in twist of the filament causes the bundle to extend.

metric, leading to the formation of a tail trapped in the host cytoskeleton. As polymerization proceeds at the membrane-associated end, the resulting stresses lead to movement of the bacterium. A major step in studying this type of engine has been the reconstitution of motility using silicon spheres or pure proteins (*37*, *38*).

Similar studies on cell motility have uncovered many parallels with the acrosome reaction and *Listeria* movements, including biased growth of filaments and the role of membrane-associated assembly factors and actin binding proteins Arp 2/3 and ADF. Exquisite light and electron microscopy studies (*39*) have revealed the organization of filaments in the meshwork. One feature of the meshwork is the orthotropic orientation of filaments with respect to the membrane at the leading edge of a cell. Estimates of the forces exerted by actin filaments suggest that polymerization is sufficient to extend the plasma membrane (*40*).

Other polymers also cause substantive movements through similar mechanisms. The amoeboid crawling movements of nematode sperm are driven by the polymerization of the major sperm protein (MSP). MSP, a 24-kD protein, forms a helical filament that self-associates into subfibers of a filamentous network (*41*). Assembly takes place at the cell membrane by the addition of MSP subunits thought to be dimers. The rate of polymerization, 1 μm/s, approximates the rate of cell extension. The assembly mechanism involves membrane vesicles (Fig. 3C) and ATP, although MSP does not bind ATP and can polymerize in the presence of ethanol. This suggests that energy from the hydrolysis of nucleotides does not drive the reaction, and may be derived from an unknown step at the membrane. Though the filaments are not polar, the requirement for assembly at the membrane confers the directionality of assembly; how a subunit is incorporated into a filament at the membrane remains unknown, leaving this critical step in the operation of the engine unresolved (*42*).

In principle, all filamentous polymers are potential ratchets because the dynamics of a polymer is dominated by viscous forces and thermal fluctuations at the molecular level, and Brownian motion of filaments can be rectified mechanically (*34*). Filament fluctuations eventually allow for the addition of a monomer, which effectively prevents the obstacle from diffusing backward. This action is similar to the physical operation of a mechanical ratchet. Thus motion becomes biased and leads to an effective velocity and an associated force. Because the force generated by a single filament is minuscule, being limited by the buckling threshold, we need to understand how filaments act cooperatively in a bundle to generate force on an object. On the mesoscale, the asymmetric mechanical stress on the object caused by the asymmetry of growth of the polymer network on the bacterium can lead to motion (*43*). However, the crucial step of connecting the microscopic picture to the mesoscopic one remains an open question.

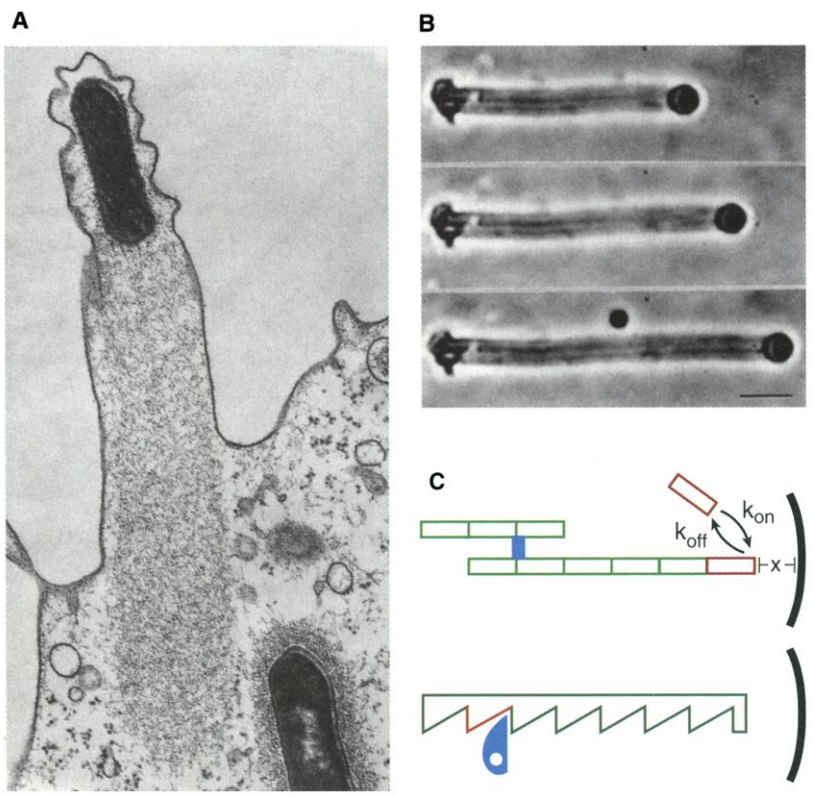

Fig. 3. Movements caused by ratchets. (**A**) Polymerization from one end of an actin bundle provides the force that propels a 2.5-μm-long *Listeria* bacterium (black oblong) through the cell surface (*35*). (**B**) In an in vitro system, a polymerizing bundle of MSP filaments moves a membrane vesicle. Scale bar, 5 μm (*54*). (**C**) A mechanical ratchet consists of a pawl (blue) and ratchet (red) that work against a load (black). The pawl and the asymmetry of the rachet rectify motion into a unidirectional movement. An anchored filament is a pawl that converts unidirectional polymerization—the ratchet—into movement against a load.

Emergent Themes

Supramolecular springs and ratchets are commonplace in biological systems and serve in a variety of functions ranging from avoidance and infection mechanisms to whole-body motion and mitosis. An emerging theme is the ability of the linear geometry of polymer subunits to magnify small conformation changes and growth into large and rapid movements. The geometry can take the form of weakly ordered or disordered structures, as in the spasmoneme or the *Thyone* acrosome, or be highly regular and crystalline, as in the case of the microtubules or the *Limulus* sperm acrosome. From a functional viewpoint, this difference is due to the large disparity between the mechanical properties of the individual filaments; actin filaments are very flexible and cannot generate large forces except in a bundle, whereas microtubules are sufficiently stiff to generate these forces alone. Because some aspects of the active kinetics of polymerization-induced growth are structure-independent, to a first approximation many biomolecular ratchets are similar, even though they are based on different proteins. However, springs exhibit a conformational bistability of latched and unlatched states. Consequently, nature has evolved several designs for springs because they derive from many structurally dissimilar protein switches. Based on these examples, it is likely that biopolymers have the ability to be both springs and ratchets.

The dynamics and energetics of biological springs and ratchets are dominated by factors that are inconsequential on the large length scales that are associated with our everyday world. In a cell, viscous forces, Brownian motion, short-range hydrophobic interactions, screened electrostatics, and steric effects influence the kinetics of filament and subunit diffusion and growth. In this soft, wet, and dynamic world, structural features are dominated by filamentous and membranous objects, a constant reminder that all events at this level are mediated by interfacial interactions. The interactions are like a hand and glove, not a lock and key. Motion and force result from energy, usually a stored chemical energy, which is dynamically trans-

duced into mechanical work by macromolecular systems. However, many efforts to apply physicochemical concepts to different protein polymer machines have been hampered by the lack of information about molecular structures and the unavailability of genetic and molecular biology techniques.

Perhaps a full physicochemical understanding of a spring or ratchet will first emerge from a microtubule system. The idea that microtubule dynamics can do work was proposed by Inoue as a mechanism for chromosome separation (*44*). Later work (*45–48*) showed that a flux of subunits through a polymer (treadmilling) or dynamics at the ends of a polymer can do work. In vitro experiments involving the growth of microtubules in vesicles show that they are capable of forces approaching 5 pN (*49*). The effect of a load on the rate of depolymerization of microtubules is consistent with the action of a ratchet (*50*).

The structural basis of the instability of a microtubule may be derived from stored energy of protofilaments in the microtubule wall. During the formation of a microtubule, guanosine triphosphate bound to the tubulin subunits is hydrolyzed; this reaction is thought to induce a conformation change that leads to curved protofilaments. Lateral contacts between protofilaments stabilize a normal microtubule; however, the end of a microtubule has a frayed appearance from the bared protofilaments (*51*). Thus, a microtubule protofilament is a spring that indirectly stores mechanical strain energy. The strain modifies the kinetics of polymerization and depolymerization, in particular by reducing the relative activation energy barrier, and thus changes the dynamics of force generation. With new structural, kinetic, and mechanical information, we may not be too far away from the goal of coupling molecular structure to function through dynamics.

References and Notes

1. A. v. Leeuwenhoek, *Philos. Trans. R. Soc. London Ser. B.* **12**, 133 (1676).
2. An engine is a device that converts one form of energy to another. A muscle is a mechanochemical engine; rhodopsin is a photochemical engine.
3. Because springs convert some form of energy to mechanical motion, a natural basis for their understanding arises from the thermodynamics of these systems. By combining the first and second laws of thermodynamics, we can relate the internal energy dU of a system to the work dW done by it and to the change in entropy dS, by $dU = TdS - dW$. The work done dW can arise from many causes; if a system expands by a volume dV against a pressure p, it does mechanical work equal to pdV. If a contractile fiber shortens by an amount $-dl$ under a force f, it performs mechanical work equal to $-fdl$. If the system transports $-dn_i$ moles of the i^{th} component from itself to its surroundings at a chemical potential μ_i, it performs chemical work equal to $-\mu_i dn_i$ etc., so that

$$dU = TdS - pdV + fdl + \sum_i \mu_i dn_i + \psi de + \ldots.$$

To determine the force generated by mechanochemical springs such as the spasmoneme and the *Limulus* acrosome, one would need to consider only the subset of relevant terms that contribute to that particular system. For example, energetic and entropic effects associated with contracting filaments lead to

$$f = \left(\frac{\partial U}{\partial l}\right)_{e,T,n_i} - T\left(\frac{\partial S}{\partial l}\right)_{e,T,n_i}$$

where e, T, and n are constant. In principle, we can calculate U, μ, and S from a microscopic description or write a phenomenological form based on the symmetries of the system. Using this force in the equation of motion for the contraction of the fiber, complemented by structural information, leads to a physicochemical description of the dynamics.

4. W. B. Amos, *Nature* **229**, 127 (1971).
5. Y. Moriyama, S. Hiyama, H. Asai, *Biophys. J.* **75**, 487 (1998).
6. Y. Moriyama, H. Okamoto, H. Asai, *Biophys. J.* **76**, 993 (1999).
7. A. Katchalsky, S. Lifson, I. Michaeli, M. Zwich, in *Contractile Polymers* (Pergamon, London, 1960), pp. 1–40
8. H. Hoffmann-Berling, *Biochim. Biophys. Acta* **27**, 247 (1958).
9. J. J. Maciejewski *et al.*, *J. Eukaryot. Microbiol.* **46**, 165 (1999).
10. Soft materials are those that deform easily and in which thermal fluctuations–induced disorder coexists with some crystalline order. Examples include polymers, colloids, and gels.
11. Y. Li and T. Tanaka, *Annu. Rev. Mat. Sci.* **22**, 243 (1992).
12. M. Shahinpoor, Y. Bar-Cohen, J. O. Simpson, J. Smith, *Smart Mat. Struct.* **7**, R15 (1998).
13. J. L. Salisbury, *J. Eukaryot. Microbiol.* **45**, 28 (1998).
14. A. Paoletti, M. Moudjou, M. Paintrand, J. L. Salisbury, M. Borens, *J. Cell Sci.* **109**, 3089 (1996).
15. D. S. Sullivan, S. Biggins, M. D. Rose, *J. Cell Biol.* **143**, 751 (1998).
16. L. Tilney, *J. Cell Biol.* **64**, 289 (1975).
17. D. J. DeRosier, L. G. Tilney, P. Flicker, *J. Mol. Biol.* **137**, 375 (1980).
18. M. B. Sherman et al., *J. Mol. Biol.* **294**, 139 (1999).
19. S. Sun, M. Footer, P. Matsudaira, *Mol. Biol. Cell* **8**, 421 (1997).
20. M. Way, M. Sanders, C. Garcia, J. Sakai, P. Matsudaira, *J. Cell Biol.* **128**, 51 (1995).
21. A. McGough, B. Pope, W. Chiu, A. Weeds, *J. Cell Biol.* **138**, 778 (1997).
22. F. Arisaka, S. Takeda, K. Funane, N. Nishijima, S. Ishii, *Biochemistry* **29**, 5057 (1990).
23. D. L. Caspar, www.sb.fsu.edu/~caspar/animation.
24. ———, *Biophys. J.* **32**, 103 (1980).
25. M. Muller, A. Engel, U. Aebi, *J. Struct. Biol.* **112**, 11 (1994).
26. C. S. Peskin, G. M. Odell, G. Oster, *Biophys. J.* **65**, 316 (1993).
27. R. Feynman, *The Feyman Lectures on Physics* (Addison-Wesley, Reading, MA, 1963–1965), vol. 1.
28. Thermal fluctuations of molecules arise due to their thermal energy $kT/2$ per molecular degree of freedom, where k is the Boltzmann constant and T is temperature. When referring to small particles that move randomly in a fluid, they are also known as Brownian motion. The balance between viscous forces and thermal fluctuations leads to an expression for the diffusion coefficient $D = kT/\nu a$, where a = size of the object and ν = kinematic viscosity.
29. The action of a ratchet-based engine is described by a Fokker-Planck–like equation for the evolution of the probability distribution of polymer lengths due to growth and diffusion (*26*). For simplicity, we ignore the structure of a bundle and consider the growth of a single linear polymer pushing against an obstacle (Fig. 3C). Then the probability $p_n(x,t)$ that the polymer is an n-mer with a gap x between its tip and the obstacle at a time t is determined by the evolution equations,

$$\frac{\partial p_n(x,t)}{\partial t} = -\frac{\partial J_n(x,t)}{\partial x} - k_{on}A_1[p_n(x,t)H(x-\delta) - p_{n-1}(x+\delta,t)] + k_{off}[p_{n+1}(x-\delta,t) - p_n(x,t)], \quad n \geq 1$$

$$\frac{\partial p_0(x,t)}{\partial t} = -\frac{\partial J_0(x,t)}{\partial x} - k_{on}A_1[p_0(x,t)H(x-\delta)] + k_{off}[p_1(x-\delta,t)]$$

where $J_n(x,t) = -D\frac{p_n(x,t)}{\partial x} + \frac{FD}{kT}p_n(x,t)$

The equation contains a kinetic (reaction) term associated with the growth of an n-mer with an on-rate k_{on} at a concentration of monomers A_1 and an off-rate k_{off} and a diffusive term. Subunits can bind only if the gap x between the obstacle and the growing polymer is larger than the subunit size δ. This condition explains the presence of the Heaviside function $H(x-\delta)$, which vanishes when $x - \delta \leq 0$ and is unity when $x - \delta > 0$. The diffusive flux $J_n(x,t)$ has two contributions; one due to the diffusion of the obstacle or the thermal bending of the filament with diffusion constant D and another due to the drift under the influence of a force F, which leads to a velocity FD/kT in the Archimedean world of low Reynolds number flows that dominate most small-scale phenomena. Growth constantly competes with diffusion and their time scales differ; the slower of these two processes limits the rate of polymerization and force production.

30. L. Tilney, S. Hatano, H. Ishikawa, M. Mooseker, *J. Cell Biol.* **59**, 109 (1973).
31. L. Tilney and N. Kallenbach, *J. Cell Biol.* **81**, 608 (1979).
32. M. K. Shaw and L. G. Tilney, *Proc. Natl. Acad. Sci. U.S.A.* **96**, 9095 (1998).
33. D. J. Olbris and J. Herzfeld, *Biophys. J.* **77**, 3407 (1999).
34. G. Oster, A. Perelson, L. Tilney, *J. Math. Biol.* **15**, 259 (1982).
35. L. Tilney and D. Portnoy, *J. Cell Biol.* **109**, 1597 (1989).
36. J. Theriot, T. Mitchison, L. Tilney, D. Portnoy, *Nature* **357**, 257 (1992).
37. L. A. Cameron, M. J. Footer, A. v. Oudenaarden, J. A. Theriot, *Proc. Natl. Acad. Sci. U.S.A.* **96**, 4908 (1999).
38. T. Loisel, R. Boujemaa, D. Pantaloni, M. Carlier, *Nature* **401**, 613 (1999).
39. T. M. Svitkina and G. G. Borisy, *J. Cell Biol.* **145**, 1009 (1999).
40. V. C. Abraham, V. Krishnamurthi, D. L. Taylor, F. Lanni, *Biophys. J.* **77**, 1721 (1999).
41. M. Stewart, K. King, T. Roberts, *J. Mol. Biol.* **243**, 60 (1994).
42. T. M. Roberts and M. Stewart, *Int. Rev. Cytol.*, in press.
43. V. Noireaux *et al.*, *Biophys. J.* **78**, 1643 (2000).
44. S. Inoue, in *Primitive Motile Systems in Cell Biology*, R. D. Allen and N. Kamiya, Eds. (Academic Press, New York, 1964), pp. 498–549.
45. A. Wegner, *J. Mol. Biol.* **108**, 139 (1976).
46. T. J. Mitchison and M. Kirschner, *Nature* **312**, 237 (1984).
47. R. L. Margolis and L. Wilson, *Nature* **293**, 705 (1981).
48. T. L. Hill and M. W. Kirschner, *Int. Rev. Cytol.* **78**, 1 (1982).
49. M. Dogterom and B. Yurke, *Science* **278**, 856 (1997).
50. A. Mogilner and G. F. Oster, *Eur. Biophys. J.* **28**, 235 (1999).
51. I. M. Janosi, D. Chretien, H. Flyvbjerg, *Eur. Biophys. J.* **27**, 501 (1998).
52. H. Stebbings and J. S. Hyams, *Cell Motility* (Longman, London, 1979).
53. D. J. DeRosier, L. G. Tilney, E. M. Bonder, P. Frankl, *J. Cell Biol.* **93**, 324 (1982).
54. J. J. Italiano, T. Roberts, M. Stewart, C. Fontana, *Cell* **84**, 105 (1996).
55. J. E. Molloy, J. E. Burns, J. Kendrick-Jones, R. T. Treagar, D. C. White, *Nature* **378**, 209 (1995).
56. S. M. Block, *Cell* **93**, 5 (1998).
57. R. Nicklas, *Annu. Rev. Biophys. Biophys. Chem.* **17**, 431 (1988).
58. D. J. DeRosier, *Cell* **93**, 17 (1998).
59. R. M. Berry and J. P. Armitage, *Adv. Microb. Physiol.* **41**, 291 (1999).
60. L. Tilney and S. Inoue, *J. Cell Biol.* **93**, 820 (1982).

61. We thank our colleagues, particularly H. Asai, C. Brokaw, J. Howard, and T. Roberts, for their comments and suggestions. L.M. thanks the California Institute of Technology for providing a warm environment during the gestation of this review. Supported by NIH grant GM52703.